

Validation of bioactive components from traditional Chinese medicine for lifespan extension

Chin-Chuan Chen (✉ chinchuan@mail.cgu.edu.tw)

Chang Gung University <https://orcid.org/0000-0002-8938-3209>

Tong-Hong Wang

Chang Gung University of Science and Technology <https://orcid.org/0000-0001-9248-9031>

Wei-Che Tseng

Chang Gung University

Yann-Lii Leu

Chang Gung University

Chi-Yuan Chen

Chang Gung University of Science and Technology

Wen-Chih Lee

The Children's Hospital of Philadelphia <https://orcid.org/0000-0001-6436-731X>

Ying-Chih Chi

Columbia University Irving Medical Center

Shu-Fang Cheng

Chang Gung University

Chun-Yu Lai

Chang Gung University

Cheng-Hsin Kuo

Chang Gung University

Shu-Ling Yang

Chang Gung Memorial Hospital

Jiann-Jong Shen

Chang Gung Memorial Hospital

Sien-Hung Yang

Chang Gung Memorial Hospital

Chun-Hao Feng

Chang Gung University

Chih-Ching Wu

Chang Gung University <https://orcid.org/0000-0002-7264-9672>

Tsong-Long Hwang

Chang Gung University <https://orcid.org/0000-0002-5780-3977>

Chia-Jen Wang

Chang Gung Memorial Hospital

Shu-Huei Wang

National Taiwan University

Article

Keywords: Pharmacopeias, Mother Enrichment Program, *Psoralea corylifolia*, *Saccharomyces cerevisiae*, Corylin, Replicative Lifespan, Cellular Senescence

DOI: <https://doi.org/10.21203/rs.3.rs-121574/v1>

License:   This work is licensed under a Creative Commons Attribution 4.0 International License.

[Read Full License](#)

Abstract

In long history of traditional Chinese medicine (TCM), some single herb and complex formulas have been recorded to increase lifespan in TCM pharmacopeia. However, the mechanism of these TCMs increasing lifespan is insufficient. Here, we collected a list of TCMs from pharmacopeias for lifespan extension. By utilizing the mother enrichment program (MEP), we systematically screened these TCMs and identified a single TCM herb, *Psoralea corylifolia*, that increases lifespan in *Saccharomyces cerevisiae*. Next, twenty-two pure compounds were isolated from *P. corylifolia*, and one of the compounds, corylin, was shown to extend the replicative lifespan (RLS) by targeting the Gtr1 protein. Furthermore, in HUVECs, the RNA sequencing data showed that corylin ameliorated cellular senescence. Finally, corylin reduced the risk of death of mice fed a high-fat diet. Taken together, these findings demonstrate that corylin has long-term benefits for longevity and could be a potential treatment for age-related disease.

Introduction

Aging is an irreversible functional decline that occurs in all organisms. Emerging evidence show that senescent cell accumulation in tissues and organs deteriorates biological function and possibly contributes to aging-associated pathology [1]. Indeed, the dysregulated molecular mechanisms of aging are highly associated to aging diseases. It has been reported that pharmaceutical compounds that extend lifespan can also be used to diabetes and cardiovascular diseases [2]. Therefore, discovering antiaging drugs could provide both benefits to health aging and novel therapeutics for aging-related diseases. In the past two decades, the TOR complex and SIRT1 activities were shown to play regulatory roles in lifespan. In particular, the EGO complex regulates mTOR1 signaling in response to amino acids abundance [3]. Growth factors regulate the mTOR1 pathway through PI3K and AKT [4]. Accordingly, caloric restriction and dietary restriction are proposed to inactivate mTOR1 signaling, resulting in lifespan extension [2]. Moreover, SIRT1 has been suggested to enhance mitochondria and alter metabolic rates to increase lifespan through its HDAC activity [5]. Despite such extensive studies in the field of aging, the number of compounds that extend lifespan is very small [6].

Scientists have been eager to identify pharmaceuticals that can extend lifespan and prevent aging diseases throughout history. However, only a few compounds with such activities have been described. There are only limited means to screen lifespan-extending drugs [7, 8]. Therefore, developing feasible and efficient methods for such screenings remains an important obstacle. Of the available screening methods for lifespan-extending drugs, the SIRT1 *in vitro* assay is the most common method, as it allows relatively simple and fast data collection [9]. However, there are limitations of this method [10]. Budding yeast represents one of the simplest and widely adopted model organisms for studying aging. Relative to other systems, the lifespan of yeast can be easily quantified. Micromanipulation is the most widely used method for assessing the replicative lifespan (RLS) of yeast; however this is an impractical drug screen method due to its time consuming process and technical difficulty on analyzing lots of sample [11]. The mother enrichment program (MEP) has been developed to monitor RLS, and it provides an alternative and simple screening method for examining replicative aging from liquid culture. This method utilizes genetic

manipulation by expressing estradiol-dependent Cre recombinase (Cre-EBD78) with a daughter-specific promoter derived from SCW11 (P_{SCW11}). Two essential genes, *UBC9* and *CDC20*, were then conditionally disrupted by the Cre-lox recombination system in the daughter cells in the presence of estradiol. The daughter cells were arrested by estradiol culture; thus, plating the culture liquid onto an estradiol-free plate allows only mother cells to replicate and form colonies. This system created a novel way to monitor mother cells without daughter cell disruption [12]. Compared with micromanipulation, the MEP assay provides a relatively quick assessment of the yeast RLS, and a large sample size can be analyzed. Here, we adopted this method and used its advantages to identify lifespan extending compounds.

Several traditional Chinese medicines (TCMs) have been recorded having lifespan extension benefits in TCM pharmacopeia, such as the *Compendium of Materia Medica*, *Qianjinyaofang*, *Shennong Materia Medica*, and *Huangdi neijing*. However, the key compounds from these TCMs have not been purified, and their lifespan-extending activities have not been validated [13-16]. Here, we utilized the MEP system to identify crude extracts from one of these TCMs, *Psoralea corylifolia*, which has great potential to extend lifespan. In addition, we purified the *n*-hexane-soluble fraction of *P. corylifolia* and identified twenty-two compounds by NMR spectroscopy, FT-IR spectroscopy, UV spectroscopy and mass spectrometry. By taking advantage of the MEP assay, we validated the activities of these compounds and identified two active compounds from *P. corylifolia* that may increase lifespan: corylin and neobavaisoflavone. In addition, we demonstrated that corylin docking to GTR1 and therefore suppress the Tor1 activity, which contributes to lifespan extension.

In mammals, cellular senescence is proposed to cause physical dysfunction and exacerbate aging process [17, 18]. It is suggested that loss of DNA repair capacity, chromosome instability and telomere erosion cause cell senescence. Additionally, senescent cells produce a senescence-associated secretory phenotype (SASP) to broaden the impact by triggering the senescence process in the ambient tissue [1] {Casella, 2019 #44; Casella, 2019 #45}. Finally, senescent cells deteriorate organ function and trigger aging-related disease, even raising the risk of death [18]. We then demonstrated that corylin alleviates senescence process in HUVECs through suppressing the mTOR pathway to increase lifespan. A previous study revealed that a high-fat diet (HFD) will induce metabolic stress and accelerate senescent cell accumulation to further increase the risk of death [18]. We further demonstrate that corylin promotes longevity in aged mice under metabolic stress, which likely contributed by improving physical functions, reducing metabolic stress, and maintaining tissue functional makers.

Results

Validation of TCMs for lifespan extension

Aging research has been an active field in recent decades; however, due to the limitations regarding screening methods and the insufficient number of candidates, to date, only a few compounds have been shown to increase lifespan [19]. In the long history of Chinese medicine, some TCMs have been reported to have lifespan-extending benefits. Thus, TCMs are great candidates for screening and verifying their

life-extending properties. To choose TCM candidates for validation, we searched the National Health Insurance Research Database (NHIRD) as well as several pharmacopeias, such as the *Compendium of Materia Medica*, *Qianjinyaofang*, *Shennong Materia Medica*, and *Huangdi neijing*, for TCMs that may increase lifespan and are used to treat age-associated diseases. After cross-comparison of these TCMs and consultation with clinical TCM doctors, 33 single TCM herbs and 6 TCM herbal formulas were chosen as candidates (Table 1).

***Psoralea corylifolia* increases viability in MEP**

The mother enrichment program (MEP) was developed to monitor the RLS of mother cells from liquid cultures [12]. We first investigated whether the TCMs listed in table 1 extend the RLS of yeast using the MEP assay. Based on crude water and ethanol extractions, we generated 78 candidates from that list. Various concentrations of each sample were tested using the MEP assay (data not shown). We found that the ethanol extract of *P. corylifolia* significantly increased viability based on MEP, suggesting that the ethanol extract of *P. corylifolia* may extend the RLS of yeast (Fig. 1A).

***Psoralea corylifolia* increases the RLS of yeast**

The MEP assay offers an easy and efficient strategy for assessing yeast RLS. However, once the division rates change with the age of yeast, the TCM could distort the MEP viability curve [12]. Thus, we sought to identify whether *P. corylifolia* increases yeast RLS in a micromanipulation system. Consistent with the MEP screening, the ethanol extract of *P. corylifolia* at 10 µg/ml significantly extended the RLS by micromanipulation (Fig. 1B). *P. corylifolia* is mainly distributed throughout India and South Asia. The different distributions under different cultivation conditions could have distinct chemical constituents. To characterize *P. corylifolia*, the fingerprint of the chemical constituents in the ethanol fractions of *P. corylifolia* was determined by HPLC. Under the optimal chromatographic conditions, the major components of *P. corylifolia* were identified, and baseline separation was obtained. Figure 1C shows a representative chromatogram of the ethanol extract of *P. corylifolia*. The fingerprint derived from the HPLC assay is a reproducible and reliable method and could be used in the quality control of the preparation of active fractions of *P. corylifolia*.

***Psoralea corylifolia* promotes yeast RLS in a Tor1-dependent manner**

There are a significant number of compounds in the crude ethanol extract of *P. corylifolia*. To narrow down the candidates, we first partitioned the ethanol crude extract into *n*-hexane and water to separate the high- and low-polarity compounds. Using the micromanipulation assay, we identified that the *n*-hexane fraction of the ethanol extract of *P. corylifolia* increased the yeast lifespan by 20% at 10 µg/ml (Fig. 1D). Next, we investigated the mechanism of the lifespan-extending activity of the *n*-hexane fraction of the ethanol extract of *P. corylifolia*. In *Saccharomyces cerevisiae*, *SIR2* and *TOR1* are key players regulating the lifespan of yeast. The Sir2 protein has been well characterized as a lifespan-extension factor for replicative lifespan [20]. The *sir2Δfob1Δ* double deletion strain was used to study the genetic pathway of *sir2* [21]. Interestingly, we found that the *n*-hexane extract of *P. corylifolia* promotes the mean

lifespan of the *sir2Δfob1Δ* strain, indicating that the *n*-hexane fraction of *P. corylifolia* increases RLS via a Sir2-independent pathway (Fig. 1E). We next examined whether the *n*-hexane extract of *P. corylifolia* elevated yeast RLS through a tor1-dependent pathway. As the data show, treatment with *P. corylifolia* did not extend the RLS of the *tor1Δ* deletion strain (Fig. 1F). These data suggested that Tor1 plays a major role in the ability of the *P. corylifolia* *n*-hexane-soluble fraction to extend the RLS of *Saccharomyces cerevisiae*.

Corylin and neobavaisoflavone are the active compounds in *Psoralea corylifolia* that extend the RLS of yeast

Although we were able to verify that the *n*-hexane fraction of the ethanol extract of *P. corylifolia* contributes to RLS extension in yeast, the *n*-hexane fraction of *P. corylifolia* contains numerous constituents. To identify the active compound (s) from the *n*-hexane extract of *P. corylifolia* that increase yeast RLS, we first separated compounds in the *n*-hexane extract by column chromatography and isolated 22 pure compounds. Each of these compounds was identified by spectroscopic analyses, including 2D-NMR, FT-IR, and UV, as well as a literature survey (Fig. 2). Interestingly, compounds **15**, **16**, **17** and **18** were isolated from *P. corylifolia* for the first time. All 22 compounds were divided into three main groups: coumarins (**1-5**), benzenoids (**6**) and flavonoids (**7-22**). The flavonoid group was further divided into four subgroups according to their structure: flavanones (**7-9**), isoflavones (**10-16**), flavonol (**17**), and chalcones (**18-22**). We found that 2 of the 22 compounds, corylin (**12**) and neobavaisoflavone (**14**), significantly increased viability in the MEP system at 15 μM (Fig. 3E and F). These results showed that corylin (**12**) and neobavaisoflavone (**14**) may be the major components responsible for the lifespan-extending ability of *P. corylifolia*. Of these two compounds, corylin more effectively increased the viability of yeast in the MEP assay compared with neobavaisoflavone (Fig. 3F). In addition, neobavaisoflavone (**14**) shares the same basic skeleton as corylin with few differences. Moreover, corylin was ten times more abundant than neobavaisoflavone in the *n*-hexane fraction, suggesting that corylin is the major active constituent of *P. corylifolia*.

Corylin increases yeast RLS through the Tor pathway

To further confirm the data obtained from the MEP assay, we next examined whether corylin promotes RLS in yeast by using a micromanipulation assay. The results showed that corylin significantly increased the RLS of yeast, indicating that corylin is one of the active compounds in *P. corylifolia* that increased yeast RLS (Fig. 4A). To identify the mechanism of corylin related to lifespan extension, we next examined whether corylin exerted its effect via a Sir2- or Tor1-dependent pathway by a micromanipulation assay. As the data show, corylin promoted RLS in the *sir2Δfob1Δ* double deletion strain (Fig. 4B) and failed to increase RLS in the *tor1Δ* deletion strain (Fig. 4C), which is consistent with the data shown in Figure 1F. This result suggested that corylin extends lifespan through the Tor1-dependent pathway. Tor (mTOR complex in mammals) is a key signaling response to nutrients and modulates cell growth and metabolism. Additionally, several studies have shown that inhibiting tor1 relocates Msn2/4 from the cytoplasm to the nucleus, and promotes *PNC1* expression [22]. Pnc1 hydrolyzes nicotinamide to nicotinic

acid as a precursor in NAD⁺ salvage, which increases NAD⁺ levels, activating stress responses and increasing lifespan [23]. First, we determined whether corylin relocates Msn2 to the nucleus and further increases Pnc1 levels in yeast. Fluorescence microscopy showed that corylin relocated Msn2 in the nucleus to form foci, similar to what was seen in two conditions of calorie restriction (Fig. 4D and E). We next utilized the Pnc1-GFP strain to observe Pnc1 expression by fluorescence microscopy and Western blot analysis. Fluorescence microscopy showed that corylin significantly increased Pnc1 in a dose-dependent manner (Fig. 4F), and the Pnc1 protein expression level was significantly upregulated by corylin treatment (Fig. 4G). NAD⁺ could be indirectly promoted by Pnc1, and several studies have shown that increases in NAD⁺ itself ameliorate aging-associated diseases [24]. Thus, we assessed whether corylin elevates NAD⁺ levels. As shown in Figure 4H, NAD⁺ levels were significantly increased following corylin treatment, suggesting that tor1 signaling was inhibited by corylin treatment. Caloric restriction (CR) is a well-known strategy for extending lifespan by reducing tor1 signaling [25]. CR modifies the rate of metabolism; reduces the age-associated accumulation of oxidatively damaged proteins, lipids, and DNA; regulates gene expression; and delays aging [2]. Given the evidence linking tor1 inhibition and CR, we next investigated whether corylin increases yeast RLS by a pathway mimicking CR. In yeast, CR was performed by reducing glucose from 2% to 0.5%, and we found that CR increases RLS, as previously reported [26]. Strikingly, corylin failed to extend the RLS under CR conditions (Fig. 4I).

Corylin increases yeast RLS by targeting the Gtr1 protein

To identify the target protein responsible for the ability of corylin to increase lifespan, molecular docking analysis was conducted. The docking results were displayed by Discover Studio based on references, and we tested possible targets involved in the Tor pathway in yeast. Finally, we found that Gtr1 is a potential target of corylin. The crystal structure of yeast GTR1-GTR2 protein (PDB id: 3R7W) was docked with corylin (Fig. 5A). The docking analysis showed 3 different binding domains with the Gtr1 protein, two of which were with the N-terminus, which is the GTPase-active domain. Furthermore, over 30 poses were generated, and based on bonding type, bonding distance and the position of the corylin structure, we selected possible results. Among the results, in many poses, Trp167 and Ile166 showed potential binding with corylin (Fig. 5B). To confirm the direct interactions between GTR1 and corylin, ¹H NMR chemical shifts experiments were conducted. We designed a 10-mer peptide containing the ile166 and trp167 regions from GTR1 sequences as a probe (peptide 1). Furthermore, we excluded ile166 and trp167 to generate a GTR-negative peptide (peptide 2) to evaluate the necessity of ile166 and trp167 in GTR1 that interact with corylin (Fig. 5C). Meanwhile, we found that GTR1 (Rag A in mammals) is highly conserved across species, especially the corylin binding region that we proposed (Fig. 5D). As shown in Figure 5E, peptide 1 showed upfield resonance at 8.03, 8.06, 7.87, and 7.84 ppm and downfield resonance at 7.92, 7.94, and 8.13 ppm upon additional corylin. Interestingly, peptide 2, which excluded ile166 and trp167, showed a zero shift in the presence of corylin. This result suggested that the ile166 and trp167 residues on GTR1 are essential for corylin binding. To determine whether corylin targeting Gtr1 to inactivate TOR1 signaling results in lifespan extension, the *gtr1Δ* deletion and Gtr1 overexpression strains were subjected to micromanipulation. The RLS of the *gtr1Δ* deletion strain was increased compared to that of the WT,

and *gtr1Δ* combined with corylin did not further increase the RLS in yeast (Fig. 5F). As shown in Figure 5G, the pGAL-GTR1 strain overexpressed GTR1 protein in YEPG and impaired its expression in YEPD. In YEPD, the pGAL-GTR1 strain increased RLS, and corylin failed to further increase RLS (Fig 5H). Moreover, we found that WT slightly increased RLS in the YEPG. Most importantly, the overexpression of GTR1 decreased RLS, while the overexpression of GTR1 counteracted the lifespan extension property of corylin (Fig 5I). In conclusion, these data suggested that corylin extends RLS by blocking GTR1 activates in yeast.

Corylin ameliorates cellular senescence in HUVECs

To extend our knowledge of corylin on mammalian system, we next investigated whether corylin alleviates the senescence process in HUVECs. In mammalian cells, p21 and SA-β-gal are replicative exhaustion signatures [27]. As shown in Figure 6A, corylin increased population doubling (PDL). In the late stage of HUVECs, the p21 expression level increased without corylin, indicating cell cycle arrest. However, the p21 expression level decreased under the corylin treatment (Fig. 6B and C). Additionally, corylin decreased SA-β-gal-positive senescent cells compared with the untreated group (Fig. 6D and E). To understand the mechanism by which corylin ameliorates cellular senescence in HUVECs, we next used RNA sequencing to analyze transcriptome differences in three different groups: proliferating cells (Y), senescent cells (S) and senescent cells with corylin treatment (S+C). First, we compared the S:Y (S/Y), S+C:S (S+C/S), and S+C:Y (S+C/Y) groups to verify the transcriptome changes between them. Next, we focused on 433 shared transcripts between S/Y and S+C/S (Fig.6F). By comparing the KEGG pathway annotation, we found shared pathways between the two groups associated with cellular senescence, the cell cycle, DNA replication, and the p53 signaling pathway (Fig. 6G). We next decoded the transcriptome differences in those pathways. Numerous transcripts were shifted in S/Y, such as a reduction in cyclin protein, replication factor, DNA helicase and cell proliferation signals and an increase in SASP, indicating that HUVECs are in the senescent state (Fig. 6H). However, the transcriptomes all showed a certain level of improvement in S+C/S. Furthermore, the S+C group showed a similar pattern to that of the Y group (Fig. S1), indicating that with corylin treatment, HUVECs were more proliferative. Most importantly, we found that eukaryotic translation initiation factor 4E (eIF4E)-binding protein 1 (4E-BP1) down regulated and Rho up regulated with corylin treatment, which are the downstream mTOR1 and mTOR2 pathways respectively. Additionally, we found that corylin decreased mTOR1 and p70S6k phosphorylation in U2OS cells (data not shown). Taken together, these data were consistent with our hypothesis that corylin suppresses the mTOR pathway increases lifespan.

Corylin prolongs lifespan in aged obese mice

We next asked whether corylin increases the C57BL/6 lifespan under metabolic stress. To determine the long-term effect of corylin in C57BL/6 mice, 40-week-old mice in this study were fed a HFD or HFD plus 0.1% (w/w) corylin (HFD/C) *ad libitum* for the remainder of their lives. 4 weeks after corylin supplement (at 44 weeks of age), the survival curves of the HFD and HFD/C groups began to diverge and remained separated till the end of experiments. By 102 weeks of age, 63.3% of the HFD-fed control mice had died,

compared with 43.3% of the HFD/C-fed mice. Corylin supplement significantly increased the lifespan of aged mice fed on high fat diet (Fig. 7A). Notably, the maximum difference in the survival rate between the mice supplied with corylin and the HFD-fed mice reached 30.0% at 92 weeks. Over the course of the experiment, the food intake did not differ between the two groups, suggesting that the beneficial lifespan is exerted by corylin instead of by less caloric intake (Fig 7B). To investigate the pharmacokinetics of corylin in mice, we monitored the circulating level of corylin after oral gavage. The daily dose of corylin was calculated as 50 mg per kg bodyweight based on the food intake of mice was approximately 2 g of HFD plus corylin (0.1% w/w) per day in mice with an average body weight of 40 g. The average serum level of corylin reached 0.68 μM at 1 hr after corylin oral gavage, and remained at 0.26 μM at 15 hr (Fig. 7C). These data suggested that corylin supplement benefits to longevity in aged mice under metabolic stress. To investigate the beneficial effect of corylin supplement in age-associated functional and metabolic dysregulations. We first tested rearing behavior, including vertical activity and behavior, to evaluate corylin effect on age-related physical dysfunction in aged HFD-fed mice. Motor coordination was examined by rotarod tests, which revealed physical function of muscle strength and balance that is impaired by aging. The rearing behavior showed that HFD/C-fed mice exhibited strongly increased activity compared with HFD-fed mice (Fig. 7D). In the rotarod test, HFD/C-fed mice had better motor skills as they aged than HFD-fed mice (Fig. 7E and F). This result indicated that the age-related decline in terms of physical function is ameliorated by corylin supplement. In addition to decline in physical function, the risk of aging-associated pathology is increased during aging that reflects on multiple metabolic parameters. At the end of the experiment (102 weeks of age), we collected and analyzed fasting serum parameters in both groups of aged male mice. The fasting blood glucose, total cholesterol, low-density lipoprotein (LDL) and triglyceride (TG) levels were reduced in HFD/C-fed mice (Fig 7G and H). The corylin-mediated reduction in serum lipid parameters may ameliorate the risk factors for metabolic syndrome during aging, which benefits to overall health of aging. Next, we assessed the effects of corylin on tissue functional markers. In this analysis, lower levels of a hepatic damage marker, aspartate aminotransferase (AST), and of a marker of renal function, creatinine, were found in HFD/C-fed aged mice compared to HFD-fed aged mice, indicating that corylin supplement prevents aging-associated organ functional decline (Fig. 7H). Thus, we concluded that corylin extending lifespan by protecting against age- and obesity-associated metabolic and functional declines in aged mice. This finding indicates that daily corylin supplement could benefit to overall functionality during aging process and therefore improves quality of life.

Discussion

CR influences a wide range of fundamental processes to promote lifespan in organisms [28]. The concept of Tor signal inhibition by CR is demonstrated [29]. Yet, **the hypothesis that Sir2 contributes to CR is still controversial**. In our study, corylin significantly increased the RLS of yeast in both WT and *sir2 Δ fob1 Δ* deletion strains indicates corylin increased lifespan by a sir2-independent pathway (Fig. 4A and B). However, lifespan extending ability of corylin in *sir2 Δ fob1 Δ* deletion strains is less than in WT strain (20% vs. 10%). Therefore, we suggested that inhibition of Tor1 by corylin could activate multiple signaling

pathways to increase lifespan. In turn, when Tor signaling is inhibited, Sir2 is one of the downstream mediators that extends the lifespan of yeast. In agreement with other studies, we first hypothesized that the inhibition of Tor1 could indirectly activate Sir2. Numerous studies have strongly linked Pnc1 expression to Sir2 activity [30]. Our study demonstrated corylin suppresses TOR1 activity and upregulates its downstream *PNC1* expression in yeast. This indicates that tor1 could also be a upstream regulator of sir2 [22]. Second, we hypothesized the inhibition of Tor in the Sir2-deficient strain would activate other pathways to compensate for Sir2 function, increasing the lifespan of yeast. Sir2 plays an important role in yeast lifespan by suppressing rDNA recombination. The *sir2Δ* deletion strain shows deregulation of rDNA recombination, resulting in rapid accumulation of ERCs and a decreased lifespan of yeast [31]. However, a previous study showed that in *sir2*-deficient yeast, *tor1* inhibition activated the *MSN2/4* or *sir2* *homolog gene* (*Hst1-4*) to increase lifespan by suppressing rDNA recombination in yeast [22, 32]. Based on a previous study, Sir2 activity is subordinate to Tor1 inhibition. Without Sir2, the inhibition of Tor signaling activates multiple pathways to increase the lifespan of yeast. This finding may also justify our conclusion that corylin extends lifespan in a Sir2-independent manner.

In the past two decades, TOR signaling has been widely discussed regarding its signal reduction contributes to lifespan increase. In addition, the EGO complex has a conserved function as a regulator of TOR1 [33]. Extensive studies have shown that in the EGO complex, the Gtr1-Gtr2 complex activates TOR1 and initiates anabolic signaling. Furthermore, the loss of Gtr1 consequently decreases Sch9 phosphorylation [34]. These results indicate that Gtr1 is an important regulator of TOR1 signaling. However, the limited study has shown a potential increase in RLS by reducing Gtr1 signaling with a loose criterion, indicated by a discrepancy between a-type and α -type yeast [35]. Here, we directly show that the lifespan of the *gtr1Δ* deletion strain can be increased (Fig 5F). Most importantly, we demonstrated that corylin targets the Gtr1 protein, which inactivates TOR1 signaling to increase RLS.

Cellular senescence is characterized by loss of DNA repair capacity, chromosome instability and telomere erosion [36]. In our RNA sequencing data based on corylin treatment, histone cluster family genes and double-strand break response genes were shown to be upregulated compared with senescent cells. The cyclin-dependent inhibitor p21 contributes to cell cycle arrest. Long noncoding RNA LINC00899 and homologous recombination protein BRCA1 negatively regulate p21 expression [37, 38]. We found upregulation of LINC00899 and BRCA1 in our RNA sequencing data. Furthermore, telomerase reverse transcriptase (TERT) and KLF4, the transcription regulator of TERT, were upregulated compared with the senescence group, indicating the good integrity of telomeres [39]. Whether these pathways are related to mTOR inhibition or whether corylin has other potential targets contributing to a slower senescence process require further investigation. However, our results have clearly demonstrated the potential of corylin to ameliorate cellular senescence.

In a previous study, a HFD induced metabolic stress and accelerated senescent cell accumulation to further increase the risk of death [18]. In our animal experiment showing that corylin extends lifespan in mice fed with HFD, corylin increased survival by 20% at 102 weeks. Of note, the reduction in the risk of death was better than that produced by resveratrol in obese mice [40]. Despite extensive studies in the

field of aging, the lack of systematic methods to screen and validate lifespan extension compounds lead to very few effective compounds were identified. Here, we extract knowledge from TCM pharmacopeia, and exploited MEP to efficiently and scientifically identify lifespan-extending TCMs in yeast. Most importantly, we are the first group to report that *P. corylifolia* and one of its major constituents, corylin, extend lifespan in various models. Moreover, the molecular mechanisms of aging are highly related to aging diseases. Consistent to our findings, our previous study revealed that corylin inhibits vascular cell inflammation, proliferation, migration and reduces atherosclerosis in ApoE-deficient mice, indicating that corylin has the potential to treat aging-associated diseases [41]. In addition, we previously showed that corylin improves obesity by activating white adipocytes browning and ameliorate insulin resistance in diet-induced obesity (DIO) mice [42].

In conclusion, we have proposed an efficient method for screening and validating beneficial compounds to extend lifespan, with strong evidence showing the lifespan extension properties of corylin in multiple organisms.

Declarations

Acknowledgments

We are grateful for the generous gift of yeast strains from Jessica Tyler and Dan Gottschling. We thank the staff of the Taiwan Yeast Bioresource Center at the First Core Labs, National Taiwan University College of Medicine, for bioresource sharing. This work was supported by grants from Chang Gung Memorial Hospital (CMRPD1K0381) and the Ministry of Science and Technology (109-2628-B-182-007) of Taiwan.

Author Contributions

Conceived and designed the experiments: Chin-Chuan Chen, Shu-Huei Wang and Yann-Lii Leu, Wen-Chih Lee, Ying-Chih Chi; performed the experiments: Wei-Che Tseng, Tong-Hong Wang, Cheng-Hsin Kuo, Shou-Chen Liu, Chi-Yuan Chen and Shu-Fang Cheng; analyzed the data: Chin-Chuan Chen, Chih-Ching Wu, Yann-Lii Leu, Chun-Hao Feng, Shu-Ling Yang, Jiann-Jong Shen, Hsien-Hung Yang and Chia-Jen Wang; contributed reagents/materials/analysis tools: Chi-Yuan Chen and Tsong-Long Hwang; and wrote the paper: Chin-Chuan Chen, Wei-Che Tseng and Chun-Yu Lai.

Competing Interests

The authors have declared that no competing interests exist.

Materials And Methods

Genotypes of yeast strains

Strain	Genotype	Source
By4741	MAT a his3 Δ leu2 Δ met15 Δ ura3 Δ	This study
ZHY02	MAT alpha ade2::HisG his3 leu2 met15 Δ ::ADE2 trp1 Δ 63 ho Δ ::SCW11pr-CRE-EBD78-NatMX loxP-UBC9-loxP-LEU2 loxP-CDC20-Intron-loxP-HPHMX	Tyler lab [43]
BJY02	MAT alpha ade2:: His G his3 leu2 met15 Δ ::ADE2 trp1 Δ 63 ho Δ ::SCW11pr-CRE-EBD78-NatMX loxP-UBC9-loxP-LEU2 loxP-CDC20-Intron-loxP-HPHMX fob1::kan	Tyler lab [43]
DCY05	MATa his3 Δ leu2 Δ met15 Δ ura3 Δ GFP-PNC1	This study
<i>gtr1</i> Δ	MATa his3 Δ leu2 Δ met15 Δ ura3 Δ <i>gtr1</i> ::KAN	Taiwan Yeast Bioresource Center
HSY002 (pGAL-GTR1)	MATa his3 Δ leu2 Δ met15 Δ ura3 Δ pGal-GFP-GTR1::KAN	This study

To overexpress GTR1, we used a plasmid generated by *Longtine et al* that replaced the GTR1 promoter with a regulated promoter by galactose with a GFP tag[44].

General experimental procedure

Optical rotations of compounds were measured on a JASCO P-1010 polarimeter using a 10-cm cell. UV spectra were recorded on a Hitachi UV-2010 spectrophotometer, and IR spectra were recorded on a JASCO FT-IR-4000 spectrometer. NMR spectra were recorded on a Bruker AVANCE-400. Proton and carbon NMR spectra were measured on a 400-MHz instrument. Mass spectrometry data were obtained on a Finnigan TSQ 700 mass spectrometer. HPLC separations were performed on a HITACHI L-2130 HPLC equipped with a HITACHI L-2400 refractive index detector.

Chemicals

Peptone was obtained from OXOID (LP0037; Basingstoke, UK), and yeast extract was obtained from BD (212750; Sparks, MD, USA). DMSO (D8418), estradiol (E2758-1G) and ADH (A7001-15KU) were obtained from Sigma-Aldrich (St. Louis, MO, USA), and TCA was obtained from Nippon Shiyaku Kogyo (Osaka, Japan).

TCM Materials

All of the TCMs were supplied and authenticated by the Chuang Song Zong pharmaceutical company (Pingtung, Taiwan). A voucher specimen (CGU-PC-1) was deposited in the herbarium of Chang Gung University, Taoyuan, Taiwan.

Extraction and Isolation of *P. corylifolia* The dried fruits (5.4 kg) of *P. corylifolia* were repeatedly extracted with ethanol (11 L \times 4) and extracted 5 times with ethanol at 70°C for 4 hr (11 L \times 5). The combined crude

extracts (1.4 kg) were partitioned sequentially between H₂O (842.38 g) and n-hexane (557.62 g). The wet n-hexane layer was separated by silica gel chromatography using sequential mixtures of hexane and ethyl acetate. The 20:1=H:E mixture eluted **6**; the 10:1=H:E mixture eluted (in order of elution) **1, 2, and 7**; the 7:1=H:E mixture eluted (in order of elution) **5, 8, 9, 11, 13, and 18**; the 5:1=H:E mixture eluted (in order of elution) **12, 14, 15, 16, and 17**; and the 1:1=H:E mixture eluted (in order of elution) **3, 4, and 10**.

Mother enrichment program (MEP)

The liquid aging assay was performed as previously described [12]. Briefly, cells were cultured at 30°C in YEPD medium overnight, and the cultures were diluted to $A_{600}=0.25$ and recovered to the log phase.

Cultures were counted and inoculated in culture tubes at a cell density of 2×10^3 cells/ml. The mixtures contained 17 β -estradiol at a final concentration of 1 μ M, and they were incubated in a roller drum at 50 rpm and 30°C for 60 hr. Each group was monitored by harvesting samples at the indicated time points. The collected samples were washed and plated in solid media, and the viability is reported as CFUs per 500 μ l.

Micromanipulation assay

The micromanipulation of the yeast cells was carried out as described previously [45]. Prior to analysis, strains were plated onto fresh solid medium and grown for 2 days at 30°C. Single colonies were grown in YEPD medium overnight at 30°C, and a small number of cells were then plated onto a fresh YPD plate for lifespan analysis. After overnight growth on the lifespan plates, the cells were arrayed on the plate using a micromanipulator and allowed to grow for approximately 3 hr. Virgin daughter cells were selected and subjected to lifespan analysis. In the lifespan experiments, the plates were incubated at 30°C during the day and stored at 4°C overnight. Each experiment consisted of more than 70 mother cells and was independently repeated 3 times.

Immunoblotting

Yeast protein was prepared as previously described [46]. The samples were loaded in 10% SDS-polyacrylamide gel. The following primary antibodies were used for immunoblotting at a 1:1000 dilution: anti-Pgk1 (ab113687; Abcam, UK) and anti-GFP (G1544; Sigma-Aldrich; St. Louis). Secondary antibodies were obtained from Sigma-Aldrich (St. Louis) and used at a 1:100000 dilutions. Images were acquired with a Wealtec KETA-CL imaging system.

Intracellular NAD⁺ content

Cells were harvested (4×10^8 per group), washed with 50% DMSO and water, pelleted and stored at -80°C. The extractions were performed with 250 μ l of 1 M formic acid saturated with butanol. After incubation for 30 min on ice, 62.5 μ l of 100% TCA (W/V) was added to each sample, and the samples were then incubated on ice for an additional 15 min. The samples were pelleted by centrifugation at 17000 g for 5 min, the supernatant was transferred to another Eppendorf tube, the pellets were washed with 125 μ l of

20% TCA, and the material was pelleted by centrifugation. The combined supernatants were used for the following tests. For analysis, each sample was assembled in reaction buffer (100 μ l of extract, 400 μ l of 360 mM Tris, 240 mM lysine, pH 9.7, 0.24% (v/v) EtOH; the control group had 5 μ l of water, and the ADH group had 5 μ l of 5 mg/ml alcohol dehydrogenase). After 5 min at room temperature, the absorbance of each sample was measured at 340 nm. The NAD⁺ content of the cells in each sample was determined relative to the water group (as the basal NADH level) and the alcohol ADH catalytic group.

Fluorescence microscopy

Yeast cells were recovered twice to the log phase in YEPD. For the Msn2 relocation assay, Msn2-GFP cells were cultured in 1 ml of culture liquid in a microtube for 1.5 hr in a rolling drum. The samples were washed with 100 mM HEPES and stained with Hoechst (#33342; Sigma-Aldrich; St. Louis, MO, USA) containing 3.7% formaldehyde for 5 min at room temperature. The samples were washed twice with HEPES and spotted onto slides for observation. The Pnc1-GFP strain was harvested, and 2×10^7 cells were washed twice with YEP. Each group was collected for further analysis by a Nikon ECLIPSE Ni-U plus fluorescence microscope equipped with a 100x oil objective. Images were acquired with a DS-U3 CCD camera and controlled using NIS-Element BR 4.0 software.

Molecular docking analysis

The crystal structure of yeast Gtr1-Gtr2 was used for analysis (PDB ID: 3R7W). The docking analysis was performed using BIOVIA Discovery Studio v19.1.0.18287. The protein was prepared, and the ligand was minimized before docking. Docking was performed using the standard protocol.

Chemical shift experiment

NMR binding experiments were carried out with peptide substrates, which included the GTR1 peptide Ile-Gly-Thr-Ser-Ile-Trp-Asp-Glu-Ser-Leu. ¹H NMR spectra were recorded on a 400-MHz Bruker DRX spectrometer equipped with a TXI cryoprobe at 25°C. Data sets were the average of 100 scans. All NMR spectra were collected in the presence of peptide, corylin, and 99.9% DMSO-d₆.

Cell culture

HUVECs were kindly provided by Professor Shu-Huei Wang of College of Medical, National Taiwan University Department of Anatomy and Cell Biology (Taiwan). HUVECs were cultured in M199 supplemented with HEPES, ECGS (Millipore), heparin, NaHCO₃, L-glutamine, sodium pyruvate, and FBS (20% final concentration). The cells were grown in an atmosphere of 5% CO₂ at 37°C and sub-cultured by trypsinization with trypsin-EDTA (Lonza). Cells were seeded at 8×10^4 in 3.5-cm culture dishes and passaged such that the monolayers never exceeded 90% confluency. A sample was collected in every passage for cell extraction, RNA extraction and SA- β -gal staining. The cells were propagated until senescence, and cell numbers were determined when sub-cultured. Population doublings (PDs) were

estimated using the following equation: $PDL = 3.32 (\log (\text{total viable cells at harvest}/\text{total viable cells at seeding}))$.

SA- β -gal staining

HUVECs were treated with or without corylin. Then, when the cells reached 90% confluency, they were washed twice with phosphate-buffered saline (PBS) and fixed for 5 min with 2% formaldehyde and 0.2% glutaraldehyde. The cells were then incubated at 37 °C for 18 hr with a staining solution (40 mmol/L citric acid, sodium phosphate, pH 6.0, 1 mg/mL 5-bromo-4-chloro-3-isolyl- β -D-galactoside (X-gal, Sigma), 5 mmol/L potassium ferrocyanide, 5 mmol/L potassium ferricyanide, 150 mmol/L NaCl, and 2 mmol/L $MgCl_2$). Senescence-associated (SA)- β -gal-positive cells were observed by microscopy, and over 300 cells were counted in three independent fields.

RNA sequencing

RNA was collected from HUVECs and extracted by TRIzol (T9424, Sigma, USA). The extracted RNA samples were sent to Genomics (Taipei, Taiwan) for analysis, and a library was constructed. Briefly, after quality control of raw reads, mRNA was purified using reverse transcriptase and a random primer to synthesize single-strand cDNA, and dUTP was used in place of dTTP to generate double-stranded cDNA. A single 'A' nucleotide was added to the 3' end of ds cDNAs. Then, multiple indexing adapters were ligated to the 5' and 3' ends of ds cDNA. PCR was used to selectively amplify the DNA fragments with adapters on both ends. The library was validated on an Agilent 2100 Bioanalyzer and Real-Time PCR System. The gene ratio and expression change were summarized by Kyoto Encyclopedia of Gene and Genomes (KEGG) pathway data and Gene Ontology (p-value <0.05, log-2 > 2).

Animals

C57BL/6 mice (34 weeks of age) were provided by the National Laboratory Animal Center (NLAC), NAR Labs, Taiwan. All mice were housed in individual cages and maintained at room temperature at $23 \pm 1^\circ\text{C}$ with a 12-hr dark/light cycle. All animal procedures were approved by Chang Guan University Animal Care Center (IACUC protocol no. CGU15-150). After reaching 40 weeks of age, the mice were randomly divided into two groups: Group I (HFD), fed a HFD with 54% fat (Table 1) (n=30), and Group II (HFD/C), fed a HFD containing corylin (1 g corylin/1 kg HFD) (n=30). Corylin (purity $\geq 98\%$) was purchased from Shanghai BS Bio-Tech Co., Ltd., China.

	HFD	HFD/C	
	g/kg diet		Source
Casein	254	254	Sigma
Cellulose	61	61	Sigma
Sucrose	321	321	General Stores
Soybean oil	10	10	General Stores
Unsalted butter	290	290	General Stores
AIN-93G Mineral mixture	44.5	44.5	MP Biomedicals
Ain-93 Vitamin mixture	12.5	12.5	Dyets, Inc.
L-Cystine	4	4	Sigma
Choline bitartrate	3	3	Sigma
Corylin	-	1	Shanghai BS Bio-Tech
kcal/g	5.016		
CHO calorie/total calories (%)	25.7		
Fat calorie/total calories (%)	54.0		
Protein calorie/total calories (%)	20.3		

Pharmacokinetic analysis

Blood samples were collected at 1, 3, 6, 9, 12 and 15 hr after corylin oral gavage, and serum samples were then separated. Serum samples (100 μ l) were mixed with ice-cold acetonitrile (150 μ l) at 4°C for 1 hr and then centrifuged for 15 min at 15,000 \times g and 4°C. After centrifugation, the supernatant (150 μ l) was harvested in a new Eppendorf tube, and 150 μ l of ddH₂O was added. The sample was analyzed by an LC/FTMS system.

Fasting blood glucose level

To determine the blood glucose, mice were fasting for 16 hr. The blood samples were obtained by cutting the tip of tail and the blood glucose was measured by ACCU-CHEK (Roche).

The rotarod test

Mice were tested on a rotarod at 81 weeks of age. The mice were habituated for 3 days, during which they were placed on the rotarod at a constant speed (4 rpm) and had to remain on the rotarod for 1 min every day. Testing on each day consisted of 5 trials with a 10 min rest between each trial. The acceleration trial began with the rotarod set at an initial rate of 4 rpm, accelerating to a maximum of 40 rpm within 5 min. The constant trial began with the rotarod set at a rate of 4 rpm and lasted for a maximum of 200 s. The latency to falling was recorded, and the average latency to falling was calculated for each trial.

Rearing behavior

Rearing behavior was analyzed in obese mice fed a HFD with or without corylin for 35 weeks (75 weeks of age) using the OxyletPro System. Before the metabolic rate was monitored, the mice were individually caged for 24 hr to acclimate to the system.

Serum parameter analysis

The serum LDL, TG and total cholesterol levels were measured using specific reagent kits (Fortress Diagnostics, Antrim, Northern Ireland). The serum glucose and high-density lipoprotein (HDL) levels were measured using specific reagent kits (Randox, Antrim UK). Insulin was measured by ELISA (Mercodia, Uppsala, Sweden). HOMA-IR was calculated as the fasting insulin level (mU/L) × blood glucose level (mmol/L)/22.5. The serum AST and CK levels were measured using a Fuji Dri-Chem 4000i analyzer (Fujifilm, Tokyo, Japan).

References

1. Casella, G., et al., *Transcriptome signature of cellular senescence*. Nucleic Acids Research, 2019. **47**(14): p. 7294-7305.
2. Madeo, F., et al., *Caloric Restriction Mimetics against Age-Associated Disease: Targets, Mechanisms, and Therapeutic Potential*. Cell Metab, 2019. **29**(3): p. 592-610.
3. Hatakeyama, R., et al., *Spatially Distinct Pools of TORC1 Balance Protein Homeostasis*. Mol Cell, 2019. **73**(2): p. 325-338.e8.
4. Saxton, R.A. and D.M. Sabatini, *mTOR Signaling in Growth, Metabolism, and Disease*. Cell, 2017. **168**(6): p. 960-976.
5. Tang, B.L., *Sirt1 and the Mitochondria*. Mol Cells, 2016. **39**(2): p. 87-95.
6. Gonzalez-Freire, M., et al., *The road ahead for health and lifespan interventions*. Ageing Research Reviews, 2020. **59**: p. 101037.
7. Stephan, J., J. Franke, and A.E. Ehrenhofer-Murray, *Chemical genetic screen in fission yeast reveals roles for vacuolar acidification, mitochondrial fission, and cellular GMP levels in lifespan extension*.

- Aging Cell, 2013. **12**(4): p. 574-83.
8. Maglioni, S., N. Arsalan, and N. Ventura, *C. elegans screening strategies to identify pro-longevity interventions*. Mech Ageing Dev, 2016. **157**: p. 60-9.
 9. Cantó, C. and J. Auwerx, *Targeting SIRT1 to improve metabolism: all you need is NAD(+)?* Pharmacol Rev, 2012. **64**(1): p. 166-87.
 10. Pacholec, M., et al., *SRT1720, SRT2183, SRT1460, and resveratrol are not direct activators of SIRT1*. The Journal of biological chemistry, 2010. **285**(11): p. 8340-8351.
 11. Zimmermann, A., et al., *Yeast as a tool to identify anti-aging compounds*. FEMS yeast research, 2018. **18**(6): p. foy020.
 12. Lindstrom, D.L. and D.E. Gottschling, *The mother enrichment program: a genetic system for facile replicative life span analysis in Saccharomyces cerevisiae*. Genetics, 2009. **183**(2): p. 413-22, 1si-13si.
 13. Liao, H., L.K. Banbury, and D.N. Leach, *Antioxidant activity of 45 Chinese herbs and the relationship with their TCM characteristics*. Evid Based Complement Alternat Med, 2008. **5**(4): p. 429-34.
 14. Wan, F., et al., *Lifespan extension in Caenorhabditis elegans by several traditional Chinese medicine formulas*. Biogerontology, 2014. **15**(4): p. 377-87.
 15. He, S.B., et al., *[Study on mechanism of Salvia miltiorrhiza treating cardiovascular disease through auxiliary mechanism elucidation system for Chinese medicine]*. Zhongguo Zhong Yao Za Zhi, 2015. **40**(19): p. 3713-7.
 16. Hugel, H.M., *Brain Food for Alzheimer-Free Ageing: Focus on Herbal Medicines*. Adv Exp Med Biol, 2015. **863**: p. 95-116.
 17. Cai, Y., et al., *Elimination of senescent cells by β -galactosidase-targeted prodrug attenuates inflammation and restores physical function in aged mice*. Cell Research, 2020. **30**(7): p. 574-589.
 18. Xu, M., et al., *Senolytics improve physical function and increase lifespan in old age*. Nat Med, 2018. **24**(8): p. 1246-1256.
 19. Lucanic, M., G.J. Lithgow, and S. Alavez, *Pharmacological Lifespan Extension of Invertebrates*. Ageing Res Rev, 2013. **12**(1): p. 445-58.
 20. Lee, I.H., *Mechanisms and disease implications of sirtuin-mediated autophagic regulation*. Experimental & Molecular Medicine, 2019. **51**(9): p. 1-11.
 21. Yu, R., et al., *Cellular response to moderate chromatin architectural defects promotes longevity*. Sci Adv, 2019. **5**(7): p. eaav1165.
 22. Medvedik, O., et al., *MSN2 and MSN4 link calorie restriction and TOR to sirtuin-mediated lifespan extension in Saccharomyces cerevisiae*. PLoS Biol, 2007. **5**(10): p. e261.
 23. Imai, S.-I. and L. Guarente, *It takes two to tango: NAD(+) and sirtuins in aging/longevity control*. NPJ aging and mechanisms of disease, 2016. **2**: p. 16017-16017.
 24. Rajman, L., K. Chwalek, and D.A. Sinclair, *Therapeutic Potential of NAD-Boosting Molecules: The In Vivo Evidence*. Cell metabolism, 2018. **27**(3): p. 529-547.

25. Balasubramanian, P., P.R. Howell, and R.M. Anderson, *Aging and Caloric Restriction Research: A Biological Perspective With Translational Potential*. EBioMedicine, 2017. **21**: p. 37-44.
26. Mei, S.-C. and C. Brenner, *Calorie restriction-mediated replicative lifespan extension in yeast is non-cell autonomous*. PLoS biology, 2015. **13**(1): p. e1002048-e1002048.
27. Hernandez-Segura, A., et al., *Unmasking Transcriptional Heterogeneity in Senescent Cells*. Curr Biol, 2017. **27**(17): p. 2652-2660.e4.
28. Tucci, P., *Caloric restriction: is mammalian life extension linked to p53?* Aging (Albany NY), 2012. **4**(8): p. 525-34.
29. Johnson, S.C., P.S. Rabinovitch, and M. Kaeberlein, *mTOR is a key modulator of ageing and age-related disease*. Nature, 2013. **493**(7432): p. 338-45.
30. Howitz, K.T., et al., *Small molecule activators of sirtuins extend Saccharomyces cerevisiae lifespan*. Nature, 2003. **425**(6954): p. 191-6.
31. Sinclair, D.A. and L. Guarente, *Extrachromosomal rDNA circles—a cause of aging in yeast*. Cell, 1997. **91**(7): p. 1033-42.
32. Lamming, D.W., et al., *HST2 mediates SIR2-independent life-span extension by calorie restriction*. Science, 2005. **309**(5742): p. 1861-4.
33. Kim, J. and K.-L. Guan, *mTOR as a central hub of nutrient signalling and cell growth*. Nature Cell Biology, 2019. **21**(1): p. 63-71.
34. Binda, M., et al., *The Vam6 GEF controls TORC1 by activating the EGO complex*. Mol Cell, 2009. **35**(5): p. 563-73.
35. McCormick, M.A., et al., *A Comprehensive Analysis of Replicative Lifespan in 4,698 Single-Gene Deletion Strains Uncovers Conserved Mechanisms of Aging*. Cell Metab, 2015. **22**(5): p. 895-906.
36. López-Otín, C., et al., *The hallmarks of aging*. Cell, 2013. **153**(6): p. 1194-217.
37. Chen, Q.B., et al., *Downregulated long non-coding RNA LINC00899 inhibits invasion and migration of spinal ependymoma cells via RBL2-dependent FoxO pathway*. Cell Cycle, 2019. **18**(19): p. 2566-2579.
38. Yu, Y., et al., *RBBP8/CtIP suppresses P21 expression by interacting with CtBP and BRCA1 in gastric cancer*. Oncogene, 2020. **39**(6): p. 1273-1289.
39. Hsieh, M.H., et al., *PARP1 controls KLF4-mediated telomerase expression in stem cells and cancer cells*. Nucleic Acids Res, 2017. **45**(18): p. 10492-10503.
40. Baur, J.A., et al., *Resveratrol improves health and survival of mice on a high-calorie diet*. Nature, 2006. **444**(7117): p. 337-42.
41. Chen, C.C., et al., *Corylin Inhibits Vascular Cell Inflammation, Proliferation and Migration and Reduces Atherosclerosis in ApoE-Deficient Mice*. Antioxidants (Basel), 2020. **9**(4).
42. Chen, C.-C., et al., *Corylin reduces obesity and insulin resistance and promotes adipose tissue browning through SIRT-1 and β 3-AR activation*. Pharmacological Research, 2020: p. 105291.
43. Hu, Z., et al., *Nucleosome loss leads to global transcriptional up-regulation and genomic instability during yeast aging*. Genes Dev, 2014. **28**(4): p. 396-408.

44. Longtine, M.S., et al., *Additional modules for versatile and economical PCR-based gene deletion and modification in Saccharomyces cerevisiae*. *Yeast*, 1998. **14**(10): p. 953-61.
45. Kaeberlein, M., et al., *Regulation of yeast replicative life span by TOR and Sch9 in response to nutrients*. *Science*, 2005. **310**(5751): p. 1193-6.
46. Chen, C.C., et al., *Dihydrocoumarin, an HDAC Inhibitor, Increases DNA Damage Sensitivity by Inhibiting Rad52*. *Int J Mol Sci*, 2017. **18**(12).

Table

TCM single herbs		
<p>☐☐☐ Ligustrum lucidum Fructus Ligustri Lucidi</p>	<p>☐☐☐ Ginkgo biloba Folium Ginkgo</p>	<p>☐☐ Curcuma longa Rhizoma Curcumae Longae</p>
<p>☐☐ Pinellia ternata Pinellia Tuber</p>	<p>☐☐☐ Rubus idaeus Fructus Rubi</p>	<p>☐☐ Gastrodia elata Rhizoma Gastrodiae</p>
<p>☐☐ Cinnamomum cassia Ramulus Cinnamomi</p>	<p>☐☐ Dendrobium nobile Caulis Dendrobii</p>	<p>☐☐ Fritillaria thunbergii Bulbus Fritillariae</p>
<p>☐☐ Glycyrrhiza uralensis Radix Glycyrrhizae</p>	<p>☐☐☐ Trichosanthes kirilowii Radix Trichosanthis</p>	<p>☐☐ Poria cocos Poria</p>
<p>☐☐ Citrus aurantium Fructus Aurantii Immaturus</p>	<p>☐☐☐ Perilla frutescens Folium Perillae</p>	<p>☐☐☐ Coix lacryma-jobi Semen Coicis</p>
<p>☐☐☐ Perilla frutescens Caulis Perillae</p>	<p>☐☐☐ Epimedium brevicornum Herba Epimedii</p>	<p>☐☐☐ Polygonum multiflorum Radix Polygoni Multiflori</p>
<p>☐☐ Astragalus membranaceus Radix Astragali</p>	<p>☐☐ Eucommia ulmoides Cortex Eucommiae</p>	<p>☐☐ Polyporus umbellatus Polyporus</p>
<p>☐☐☐ Eleutherococcus senticosus Radix Acanthopanax Senticosol</p>	<p>☐☐☐ Gynostemma pentaphyllum Herba Gynostemmatis Pentaphylli</p>	<p>☐☐☐ Psoralea corylifolia Psoraleae Fructus</p>
<p>☐☐☐ Cuscuta chinensis Cuscutae Semen</p>	<p>☐☐☐ Cnidium monnieri Fructus Cnidii</p>	<p>☐☐ Oryza sativa Germinantis Oryzae Fructus</p>
<p>☐☐ Pueraria lobata</p>	<p>☐☐☐ Gentiana scabra</p>	<p>☐☐ Rheum palmatum</p>

Radix Puerariae	Gentianae Radix	Rhizoma et Radix Rhei
葛根	龙胆	地黄
Cyperus rotundus	Ziziphus jujuba	Ginkgo biloba
Cyperus Rhizoma	Semen Ziziphi Spinosae	Semen Ginkgo
TCM herbal formula		
十全大补汤	八宝地黄丸	左归丸
Shi Quan Da Bu Tang	Ba Wei Di Huang Wan	Zuo Gui Wan
还少丹	六味地黄丸	血府逐瘀汤
Huan Shao Dan	Liu Wei Di Huang Wan	Xue Fu Zhu Yu Tang

Table 1. Lists of TCM single herbs and TCM herbal formulas used to treat aging diseases and/or extend lifespan

Figures

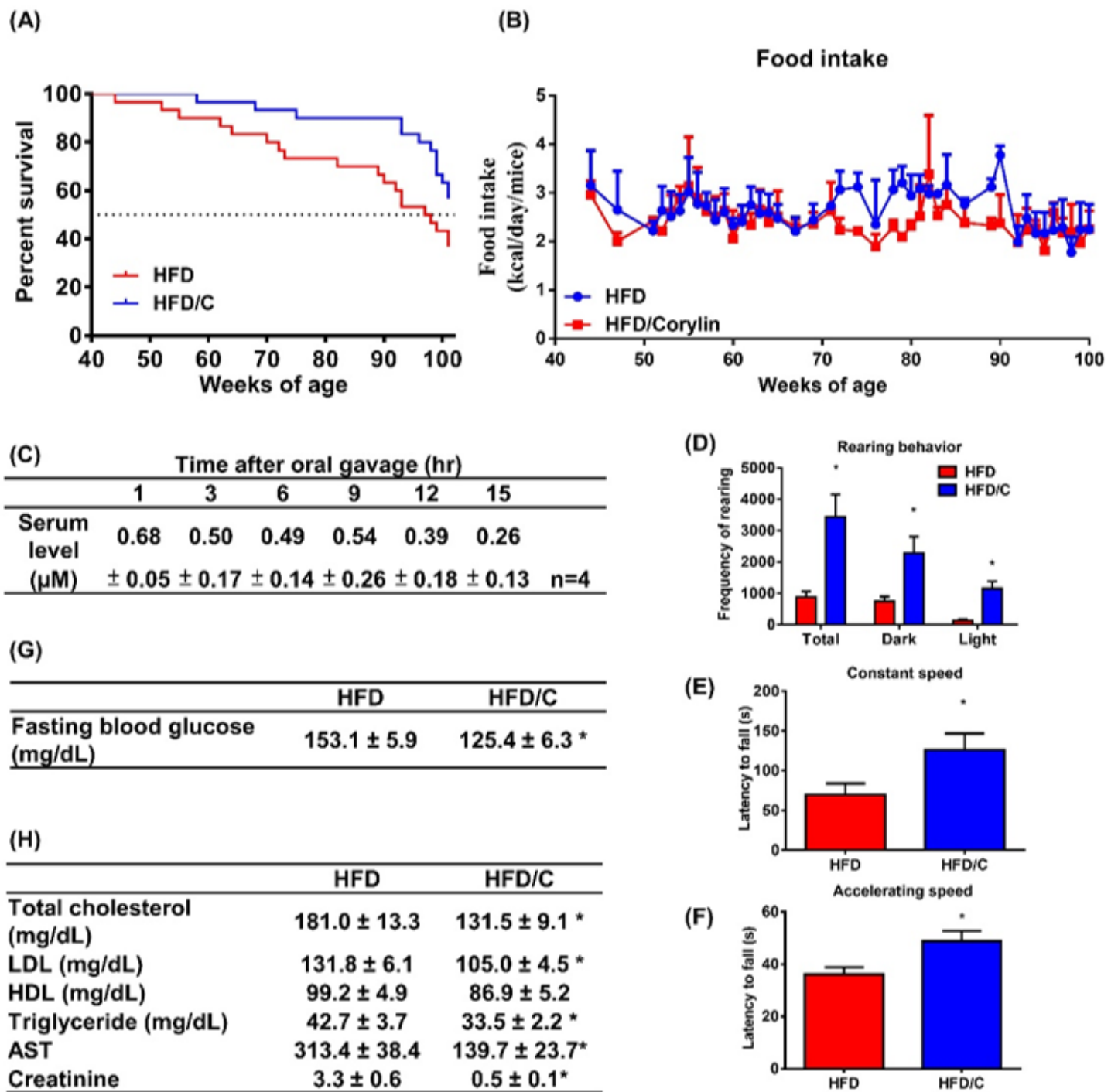


Figure 7

Corylin prolongs lifespan in aged HFD-fed mice (A) Survival curves of mice fed a HFD versus 1%(v/v) corylin (HFD/C) show a significant (Log-rank $\chi^2 = 4.887$ and $p = 0.0271$) improving lifespan (B) Food consumption. (C) Circulating level of corylin; values are expressed as the mean \pm SEM (n=4). (D) Rearing behavior was analyzed in obese mice fed a HFD with or without corylin for 35 weeks under dim and bright light conditions. n=12. Latency to falling in the (E) constant rotarod and (F) accelerating rotarod tests (HFD: n=15; HFD/C: n=12). (G) Fasting blood glucose level result (HFD: n=9; HFD/C: n=9). (F) Serum

biochemical marker results (HFD: n=10; HFD/C: n=13). Values are expressed as the mean \pm SEM. Asterisks (*) indicate significant differences between corylin-treated and untreated cells (* p <0.05).